COMPOSITION OF MAGMATIC FLUIDS IN THE HARNEY PEAK GRANITE, BLACK HILLS, SOUTH DAKOTA

A Thesis

presented to

the Faculty of the Graduate School

at the University of Missouri-Columbia

In Partial Fulfillment

of the Requirements for the Degree

Master of Science

---

by

MARK L. GRZOVIC

Dr. Peter I. Nabelek, Thesis Supervisor

MAY 2013

The undersigned, appointed by the dean of the Graduate School, have examined the thesis entitled

MAGMATIC FLUID COMPOSITION IN THE HARNEY PEAK GRANITE, BLACK HILLS, SOUTH DAKOTA

presented by Mark L. Grzovic,

a candidate for the degree of Master of Science in Geology,

and hereby certify that, in their opinion, it is worthy of acceptance.

_____

Dr. Peter I. Nabelek, Advisor

_____

Dr. Martin S. Appold

_____

Dr. Michael D. Glascock

To my mother,

Carol A. Grzovic

for her advice and support.

I wish you were here for this accomplishment.

ACKNOWLEDGEMENTS

I would like to thank my advisor, Dr. Peter I. Nabelek, for his guidance, patience, and motivation. I am grateful to Barry Higgins for his help and instruction on use of the laser ablation ICP-MS system, Dr. Martin S. Appold for his instruction and insight, and Dr. Michael D. Glascock for his advice and support. Thanks to Dr. Kevin L. Shelton for his guidance and humor. I would also like to thank all my friends and colleagues at Mizzou for their advice, strength and encouragement: Savas and Gina Ceylon, Koray Ekinci, Yanying Chen, Hal Johnson, Geneviève Robert, and many others.

Support for this thesis came from teaching assistantships from the Department of Geological Sciences and the John W. Tlapek Geology Student scholarship.

I would also like to recognize the NSF for funding the Major Research Instrument grant to the University of Missouri Research Reactor (NSF grant No. 0922374), which purchased the equipment used, and NSF grant No. EAR-0911116 that funded field work, thick sections and microthermometry.

Finally, I would like to thank my family and friends for their support and encouragement.

TABLE OF CONTENTS

LIST OF FIGURES

LIST OF TABLES

ABSTRACT

The composition of magmatic fluids influences the differentiation of magmas and the mobility of elements within igneous systems. Fluid inclusions are potential trapped samples of magmatic fluids. The composite Harney Peak granite-pegmatite pluton (HPG) in the Black Hills, South Dakota, is a good location to study the composition of trapped magmatic fluids because of its unaltered and simple mineralogy. Fluid-soluble elements such as Na, K, Li, and B are important components in leucogranites, such as the HPG, and therefore it is important to understand their concentrations in magmas and exsolved fluids. The core of the HPG consists of sills and dikes with biotite as the dominant ferromagnesian mineral, whereas tourmaline is the dominant ferromagnesian mineral in the perimeter. Previous studies of the surrounding metamorphic rocks suggest that Li enrichment in the granite's contact aureole was caused by Li-bearing fluids emanating from the HPG. Past investigations of fluid inclusions in the HPG have used bulk crush-leach methods. In this investigation, laser ablation (LA) ICP-MS analysis was used instead because it provides a way to measure the composition of individual fluid inclusions *in situ*. Fluid inclusions in quartz were measured by microthermometry and LA ICP-MS to determine the chemical composition of the magmatic fluids in the HPG system.

Three types of fluid inclusions were identified in samples of quartz from the HPG: type 1 inclusions are low-salinity aqueous-carbonic, type 2 are high-salinity aqueous, and type 3 are carbonic inclusions dominated by CO_2. Type 1 fluid inclusions are primary and occur as either single isolated inclusions, or as isolated groups of

inclusions. Type 2 and type 3 occur as secondary fluid inclusions along healed fractures and are thought to represent unmixed end-members of type 1 inclusions. Low ice freezing point depressions (as low as -35.0°C) and eutectic temperatures (as low as -58.4°C) of type 2 inclusions in biotite- and tourmaline-bearing granites indicate the presence of solutes other than Na in the inclusions. LA ICP-MS analysis confirms this with high concentrations of NaCl (up to 24.9 wt. %), KCl (up to 1.1 wt. %), and LiCl (up to 0.6 wt. %), and minor concentrations (<0.01 wt. %) of other solutes (e.g. CsCl and RbCl) in both biotite- and tourmaline-bearing granites. Inclusions in biotite-bearing granites also have high concentrations of $SrCl_2$ (up to 0.35 wt. %). In contrast, type 2 inclusions in a tourmaline-poor pegmatite, informally called the "New" pegmatite, have higher ice freezing point depressions (mean of -1.9°C) and eutectic temperatures (mean of -12.2°C) than inclusions in the tourmaline-bearing granites. These relatively elevated phase transition temperatures in the "New" pegmatite are most likely due to lower concentrations of LiCl, NaCl, KCl, and other dissolved salts (as low as 3.4 wt. % $NaCl_{eq}$). However, concentrations of B are significantly higher (up to 4.7 wt. % as H_3BO_3) in the "New" pegmatite than in the tourmaline-bearing granite (0.02 wt. % H_3BO_3 from one inclusion). Melting points for CO_2 in type 1 fluid inclusions are between -58.4°C and -56.4°C indicating that the carbonic phase is nearly pure CO_2. Concentrations of LiCl and CsCl are higher (LiCl up to 1.65 wt. %; CsCl up to 0.06 wt. %) in type 1 fluid inclusions in tourmaline-bearing granites than in type 2 inclusions hosted in these granites. In contrast, concentrations of NaCl are about the same (up to 21.69 wt. %), but KCl was not detected. Type 3 inclusions were not analyzed by LA ICP-MS because they have very little aqueous fluid.

The results of this study indicate that magmatic fluids emanating from the HPG and pegmatites contained significant concentrations of Li, and variable concentrations of B, in addition to NaCl, KCl, and other solutes. In the tourmaline- and biotite-bearing granites, magmatic fluids contained a significant amount of Na, K, and Li, but little or no B. In contrast, fluids in the "New" pegmatite contained relatively little Na in comparison to tourmaline- and biotite-bearing granites, but abundant Li, K and B. The absence of B in the higher salinity fluid inclusions in the tourmaline-bearing granites can be attributed to its scavenging by tourmaline. The high concentration of B in the low salinity fluid explains the presence of tourmaline in the metasomatic aureole of the "New" pegmatite. In addition, because B is carried as a hydroxyl species, it may have been rather insoluble in inclusions that have Cl as the dominant anion. The prevalence of B in the low salinity fluid is attributed to this speciation and low abundance of tourmaline in the "New" pegmatite. Therefore, the LA ICP-MS data provides strong evidence that in the tourmaline-bearing granites B was retained in the magma and in the "New" pegmatite B was scavenged from the magma by the low salinity fluid. The data from this study supports previous work suggesting that Li enrichments in contact aureoles of pegmatites in the Black Hills were caused by metasomatism from fluids emanating from the HPG.

INTRODUCTION

The generation of leucogranites and their associated pegmatites in the continental crust is one of the more important processes studied in petrology because it involves melting of the continental crust during collisional orogenies and transport of material in the form of melts through the crust. One of the more important aspects of the genesis of leucogranites is the role magmatic fluids play in these plutonic systems, because fluids can influence magma differentiation, density, viscosity, and the mobility of chemical species within the systems and the surrounding rocks (Lange 1994; Duke 1995; Whittington et al. 2009; Bartels et al. 2010). Fluids can also influence nucleation of crystals in the magma. Hindering of nucleation by fluid enrichment is thought to be key to the genesis of pegmatites (Nabelek et al. 2010). Nabelek et al. (2010), suggested that high water contents in magma inhibited nucleation and promoted rapid crystal growth, and that Li, B, F, and P, in sufficient concentrations, could increase this affect. In leucogranitic systems, magmatic fluids are of particular interest because of their role in the genesis of rare-element, ore-forming pegmatites. The term rare-element is use in this paper to refer to elements that usually occur as trace elements in igneous systems (e.g. Be, Sn, Nb, Ta, Cs, Li, and B). The Harney Peak granite-pegmatite (HPG) in the Black Hills, South Dakota provides an excellent location to study leucogranite systems because it's mineralogy is simple, it has not been metamorphosed, and it has not been metasomatized (Nabelek and Ternes 1997).

Although leucogranites occur in orogenic terranes of different ages from the Proterozoic (Black Hills; Dahl and Frei 1998) to the modern (Himalayan), they have

many mineralogical, chemical, and structural characteristics in common (Nabelek and Liu 2004). Leucogranites are thought to be the products of the partial melting of metapelites and metagraywackes (Nabelek and Liu 2004). They are emplaced into shallower sequences of their source rocks as a series of overlapping dikes or sills forming composite plutons (Rockhold et al. 1987; Duke et al. 1988; Duke et al. 1990; Norton and Redden 1990). Mineralogically, leucogranites are simple with the dominant minerals of plagioclase, quartz, potassium feldspar, and muscovite (Nabelek and Liu 2004). Leucogranites are characterized by the occurrence of either tourmaline or biotite. If both occur, however, in a leucogranite, they are often mutually exclusive, that is if either one occurs at a location then the other mineral is not present (Nabelek and Liu 2004). In addition, pegmatite fields are often associated with leucogranites, with many pegmatites enriched in rare-elements such as Be, Sn, Nb, Ta, Cs, Li, and B (Norton and Redden 1990). Magmatic fluids are thought to have a strong influence on the formation of these pegmatites (Nabelek et al. 2010).

Fluids influence the physical and chemical properties of both the magma and the surrounding rock. Fluids can affect both the density and the viscosity of a magma, both of which control the transport of magma through the crust (Whittington et al. 2009). Also, fluids can promote the movement of some elements (e.g. alkalis and alkali earth, transition metals) through magmas and into the surrounding rock (Duke 1995). Nabelek et al. (2010), suggested that large amounts of water dissolved in magmas can both inhibit the nucleation of crystals and, once crystals nucleate, promote rapid crystallization, and that Li, F, P, and B, in sufficient concentrations, could increase this affect. Li and B in

particular are thought to be important as fluxing components in the formation of pegmatites including rare-element pegmatites (Maloney et al. 2008).

The HPG, pegmatite field, and surrounding metapelites have been the subject of previous studies focused on understanding the evolution of the HPG, development of the pegmatite field, and formation of the metasomatic aureoles (Nabelek and Ternes 1997; Wilke et al. 2002; Sirbescu and Nabelek 2003a, 2003b). Wilke et al. (2002) analyzed the metasediments surrounding the HPG. They found enrichment of Li in the contact aureole, and hypothesized that it was caused by fluids emanating from the HPG. The studies by Sirbescu and Nabelek (2003a, 2003b) used bulk crush-leach extraction of fluid inclusions to determine the composition of the magmatic fluid. Problems with the bulk technique include possible contamination from the host mineral and difficulty in segregating multiple populations of fluid inclusions for analysis (Gleeson 2003). Laser ablation (LA) ICP-MS provides an important alternative method for determining the composition of fluid inclusions. The advantages of LA ICP-MS include the ability to determine the elemental composition of individual fluid inclusions, which allows one to target a specific population of fluid inclusions from a complex array of inclusions.

In this study, a combination of microthermometry and LA ICP-MS was used to characterize and determine the exact compositions of fluid inclusions hosted in the HPG. Microthermometry was used to identify major species (i.e. NaCl and CO_2) in inclusions that followed the classification scheme of Sirbescu and Nabelek (2003a) and to constrain the temperatures of phase transitions. The combination of these techniques provides important information on the compositions of the magmatic fluids emanating from the HPG and associated pegmatites. The goal of this study was to determine the composition

of the magmatic fluids in order to evaluate three questions: 1) Do fluid inclusions have elevated concentrations of Li and B? 2) Do secondary inclusions have different compositions than primary inclusions? 3) Do inclusions show differences in chemical composition in different parts of the HPG pluton and pegmatites? This information provides new constraints on models for leucogranite and pegmatite genesis, with connections for the genesis of rare-element pegmatites.

GEOLOGICAL SETTING

The Black Hills, located in southwestern South Dakota, is an uplifted terrane comprised of Archean and Proterozoic age metamorphic and igneous rocks (Figure 1). The terrane is dominated by various sedimentary rocks, mostly shales, graywackes, and sandstones, and gabbroic sills that were folded and thermally metamorphosed during the Black Hills orogeny (~1775-1750 Ma; Dahl et al. 2005a; 2005b). The regional metamorphism consists of dominant NNW-trending folds and the dynamothermal metamorphism up to garnet-biotite grade (Nabelek et al. 2006).

The HPG is a leucogranite intrusion located in the southern part of the Black Hills (Norton and Redden 1990). It consists of a large central pluton with smaller satellite granitic and pegmatitic plutons. The mineralogy of the HPG is simple, composed dominantly of albite, potassium feldspar, quartz, and muscovite. Two ferromagnesian minerals are also present; biotite is dominant in the core of the main pluton and tourmaline is dominant in the perimeter and satellite plutons. The HPG pluton was emplaced within schists during the Proterozoic (~1715 Ma; Redden et al. 1990; Dahl et al. 2005a) at pressures of ~3.5 – 4.5 kbar (Helms and Labotka 1991; Nabelek et al. 2006)

and temperatures up to 780°C (Nabelek et al. 1992b). A large pegmatite field surrounds the HPG. The metamorphic gradient in rocks that encompass the pegmatite field increases in

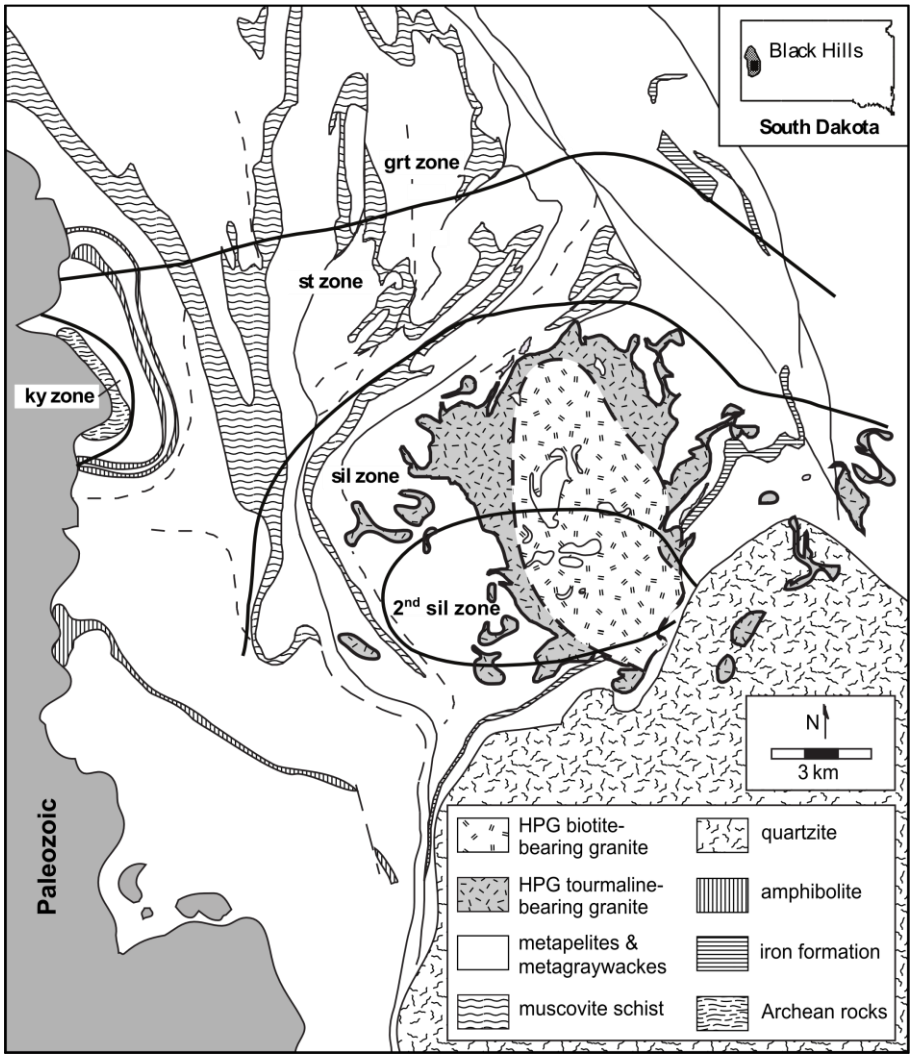

Figure 1. Geologic map of the southern Black Hills, SD. Thick lines are the approximate locations of the isograds. Thin solid and dashed lines are faults. Abbreviations: grt, garnet; st, staurolite; ky, kyanite; sil, sillimanite.

grade from the staurolite isograd up to sillimanite-potassium feldspar grade (Nabelek et al. 2006; Helms and Labotka 1991). Some of the pegmatites in the field are rich in rare-elements and contain many economically important minerals such as spodumene, lepidolite, cassiterite, and beryl (Figure 2; after Norton and Redden 1990).

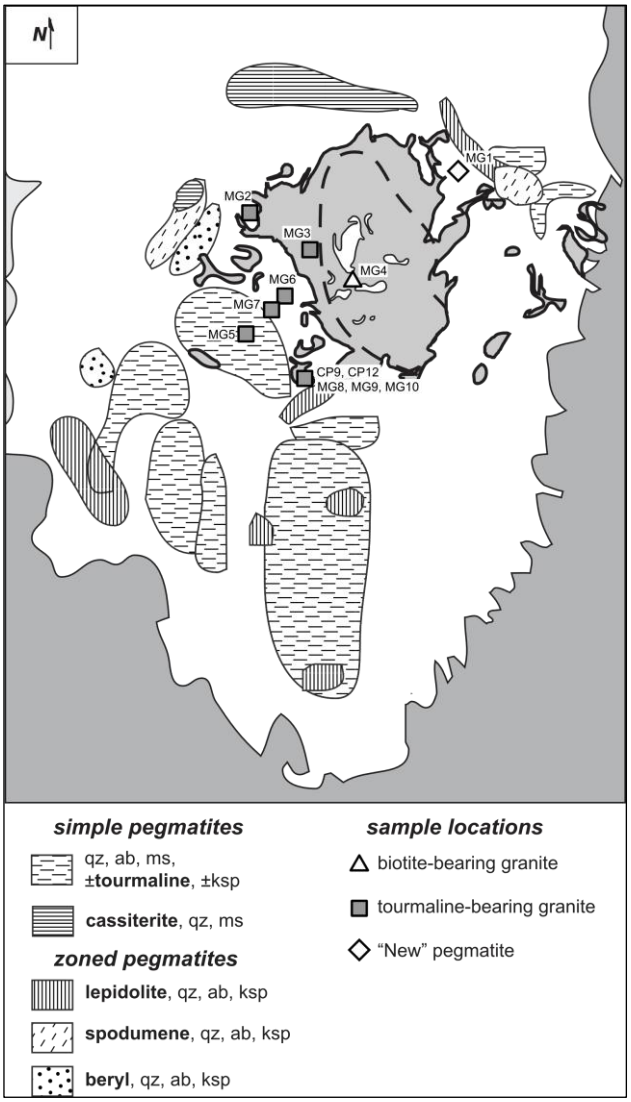

Figure 2. Map showing distribution and mineralogy of pegmatites and sample locations. Thick dashed line indicates the boundary between the biotite-bearing granite and the tourmaline-bearing granite. (after Norton and Redden, 1990)

Norton and Redden (1990) estimated that there are about 24,000 layered intrusions and pegmatites surrounding the HPG. The majority, called simple pegmatites,

contains the same minerals as the HPG, but have no internal zonation except a fine-grained chill zone (Norton and Redden 1990). Layered intrusions have similar structures and nearly the same composition as the HPG, but they are much smaller (Duke et al. 1988; Norton and Redden 1990). Zoned pegmatites are the smallest in number, but are the best documented. They are the economically important pegmatites that were mined for muscovite, Li, and Be (Norton and Redden 1990). Norton and Redden (1990) divided the zoned pegmatites into seven categories which can be placed into two groups: muscovite pegmatites (cat. 1-3) are those that are muscovite-rich, and rare-element pegmatites (cat. 4-7) that contain rare-element bearing minerals. Zoned pegmatites exhibit a weak regional zonation, with the rare-element pegmatites occurring farther from the main pluton than the muscovite pegmatites (Norton and Redden 1990).

SAMPLING AND ANALYTICAL PROCEDURES

Sample selection and preparation

Fourteen samples were selected from twelve locations around the Harney Peak Granite and associated pegmatites for microthermometry and laser ablation (LA) ICP-MS analysis. Samples were selected from three rock types based on the occurrence of ferromagnesian minerals: tourmaline-bearing granites, biotite-bearing granites, and a pegmatite with only very little tourmaline and biotite, known informally as the "New" pegmatite. Five of these samples came from the Calamity Peak pluton, a tourmaline-bearing satellite pluton, and the remaining ones came from various locations in the HPG and its satellite plutons (Figure 2). All samples were quartz, except sample HP-MG5-2, that also contained tourmaline. Doubly polished thick sections were prepared from all samples.

Microthermometry procedures

Microthermometry was performed on chips of the doubly polished thick sections using a Linkam THMSG600 heating/cooling stage housed at the University of Missouri-Columbia. The heating/cooling stage was mounted to an Olympus BX51 microscope with an attached QImaging Rolera-XR Mono Fast 1394 monochrome digital camera. This assembly was connected to a PC running the operating Linksys software. Calibration of the heating/cooling stage was performed using synthetic fluid inclusions (H_2O and a CO_2-H_2O mixture). The ice and solid CO_2 melting temperatures were within

±0.2°C of the nominal melting temperatures of the synthetic inclusions, and homogenization temperatures were within ±2°C.

Fluid inclusions were selected for microthermometric analysis based on following criteria: size, depth from surface, and location near other inclusions. Fluid inclusions chosen for analysis were limited to sizes of greater than 10 μm, and depths from the surface of less than 40 μm. The penetration distance of the laser ablation equipment used for LA ICP-MS analysis limited the maximum depth. Microthermometric measurements for inclusions outside these parameters were still obtained if the inclusions were part of a measured fluid inclusion assemblage. For aqueous inclusions, homogenization temperatures were measured first, followed by measurement of ice melting temperatures after freezing. For inclusions that were mixtures of CO_2 and H_2O, ice melting temperatures were measured first because of the increased likelihood of decrepitation upon total homogenization. This was justified based on the fact that quartz does not typically change shape readily with freezing and heating (Bodnar 2003). Phases observed during microthermometry include the following: 1) for aqueous inclusions—ice, hydrohalite, halite, water, and water vapor; 2) for carbonic inclusions—CO_2 solid, CO_2 liquid, clathrate, ice (H_2O), and CO_2 vapor. A summary of the collected microthermometry data is provided in Table 1.

Table 1. Summary of microthermometry data for tourmaline-bearing granite, biotite-bearing granite, and the "New" pegmatite.

Group	Sample	No. of analysis	Type 1					Type 2							
			T_m (°C)*	T_m (°C)*	$T_{clathrate}$ (°C)*	T_{ph} (°C)*	T_h (°C)*	T_{te} (°C)*	T_{be} (°C)*			T_m (°C)*		T_d (°C)*	T_h (°C)*
			CO_2	ice				unk†	unk†	ice	hh†	ice	hh†		
Tourmaline-bearing															
	CP-MG8-1	30	-57.2 to -56.4	-19.8 to -6.4	4.0 to 7.6	19 to 39	222 to 228								
	CP-MG10-1	20	-58.4 to -57.2		5.0 to 7.4	2 to 30	168 to 230								
	HP-MG5-2	14	-57.2 to -56.6	-10.2 to -7.0		12 to 30	132								
A	HP-MG5-2	12						-32.5			-32.4 to -31.0	-12.4 to -4.2			90 to 134
B	HP-MG5-2	11						-22.7			-22.8 to -21.4	-19.6 to -15.2			118 to 138
	CP9-3B	12							-27.1 to -21.4			-19.9 to -14.2			90 to 141
	CP12-1A	16							-24.6 to -20.6			-20.0 to -7.8			127 to 348
C	CP9-3B	25							-43.8 to -33.2			-21.4 to -16.2			82 to 106
D	CP12-1A	3							-58.4 to 56.6			-35.0 to -34.7			81 to 139
	HP-MG5-2	2									-51.0 to -50.2	-32.6 to -32.0			80
E	CP9-3B	16						-33.6 to -32.2		-22.2 to -20.8			-17.6 to -11.6		94 to 140
	CP-MG10-1	12								-21.8 to -19.8			-13.4 to -11.2		86 to 112
F	HP-MG2-1	13						-54.2 to -48.8		-25.0 to -21.6			-20.8 to -9.2		72 to 124
Misc.	CP9-3B	1								-20.3				97.0	
	CP12-1A	1												148.1	133
	CP9-3B	19													95 to 200
	HP-MG5-2	1								-23.3					89
N&T	CP		-61.5 to -57.4		5.9 to 8.4	7.9 to 24.5	240 to 380					-21.2 to -1.1			90 to 203
S&N	CP				(5.7)		(259.1)					(-14.9)			(174.6)
Biotite-bearing															
	HP-MG4-1	38									-24.0 to -21.8	-18.0 to -9.8			122 to 278
	HP-MG4-1	1									-36.5	-27.5			151
	HP-MG4-1	2										-22.5 to -22.3		8.9 to 180	118 to 300
N&T	HP											-34.7 to -3.1			78 to 347
"New" Pegmatite															
	HP-MG1-1A	29							-12.6 to -11.6			-3.4 to 0.0			140 to 180

Note: N&T—from Nabelek and Ternes (1997), S&N—from Sirbescu and Nabelek (2003a)

*T_m—final melting temp ., $T_{clathrate}$—clathrate dissolution temp., T_{ph}—partial homogenization temp., T_h—final homogenization temp., T_{te}—apparent ternary eutectic, T_{be}—apparent binary eutectic, T_d—halite dissolution temp.

†unk—unknown melting phase, hh—hydrohalite

Sample selection and LA ICP-MS procedures

After microthermometry, samples were selected for LA ICP-MS analysis by a NexION 300X ICP-MS housed at the University of Missouri Research Reactor (MURR). The laser used to ablate the samples was manufactured by Photon Machines and had a maximum energy of 15 mJ. Elements that were measured included Li, B, Na, Mg, Al, Si, K, Ca, Mn, Fe, Rb, Sr, Sn, Cs, Ba, La, Ce, W, and Os; however only some were above their detection limits. NIST 610 and NIST 612 glass standards were analyzed before and after analysis of the samples to correct for any instrument drift, which was minimal. The standards were also used to determine elemental concentrations. During analysis of the samples, the intensity of the Na mass was used to determine when fluid inclusions were opened by the laser.

One particular problem encounter during LA ICP-MS data collection was high background interference. Figure 3 shows a typical spectral signal from a fluid inclusion in tourmaline-bearing granite, and a spectral signal with high background interference for a fluid inclusion in a biotite-bearing granite. When sampling with a high background, some elements may not be detected. For example, in figure 3, there may be K in sample FI23 but it was not detected because the background was too high. The problem is encountered when the instrument is adjusted to have a high sensitivity because the level of the background is also probably high. In order to improve sensitivity for the elements being measured the operating parameters of the ICP-MS must be adjusted carefully to increase sensitivity but at the same time limit or reduce the background level.

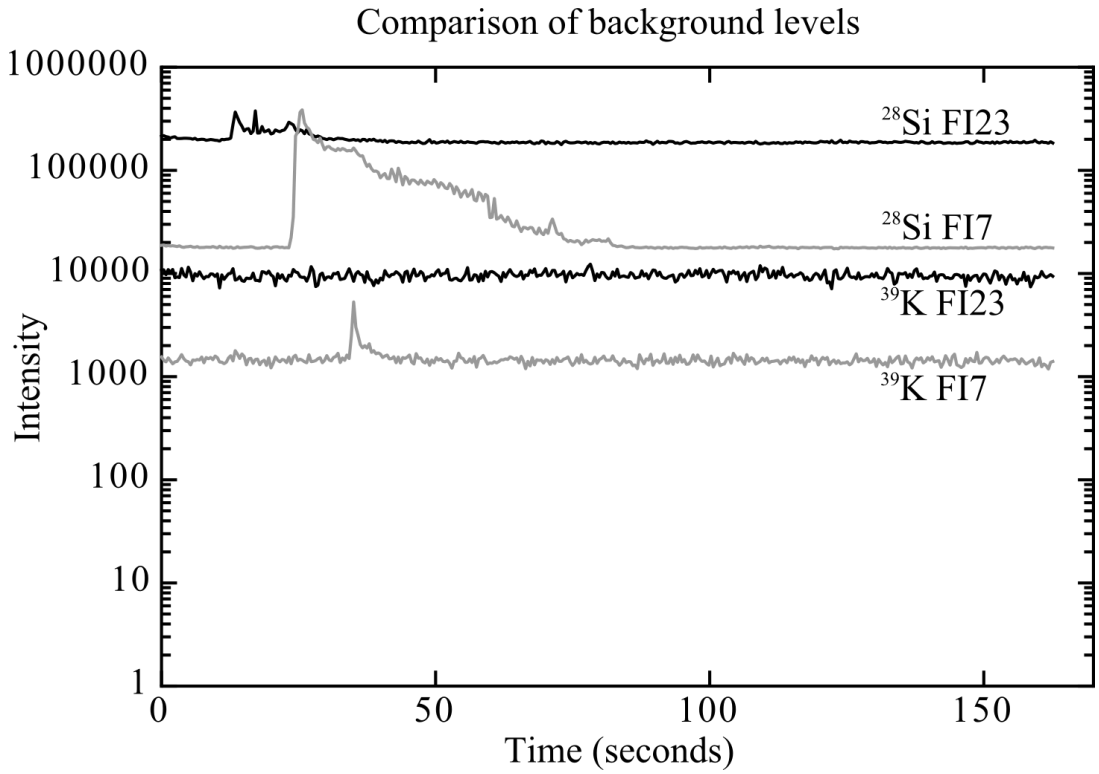

Figure 3. Time-resolved spectra from two type 2 fluid inclusions analyzed on different days. For clarity only the ^{39}K and ^{28}Si spectra are shown. The differences between the two intensities of the background illustrates the problems with adjusting the ICP-MS for maximum sensitivity.

Data reduction procedure

Raw data were reduced using the AMS 1.1.0 software obtained from the Virginia Polytechnic and State University's Fluids Research Laboratory. First, the data (dual counts) was extracted from the raw instrument data files to an Excel file using a Visual BASIC macro written by Barry Higgins at MURR. Second, the data was evaluated to determine the elements detected by subtracting the background signal, three standard deviations from the mean, and visually looking for the Na peak, which was attributed to the opening of the fluid inclusion. The concentrations of detected elements (Li, B, Na, Mg, Al, K, Rb, Cs, and W) were determined by reducing the converted data using the

AMS software. For elements that are chloride complexes, the data was reduced using Na as the internal standard (i.e. AMS microthermometry method). That is, using freezing point depressions or halite dissolution temperatures to determine salinity. For fluid inclusions containing B, Al and W, the following procedure was used instead because Al and W do not form chloride complexes but are carried as hydroxyls, and Schatz et al. (2004) has shown that in low salinity aqueous fluids H_3BO_3 is the dominant compound. The raw LA ICP-MS data was first reduced assuming elemental concentrations normalized to 100 wt. %. Then the raw data was reduced again without including B, Al or W (i.e. chloride complexes only) using the microthermometry method because the program uses total salinity ($NaCl_{eq}$) to calibrate the other element concentrations (Heinrich et al. 2003; Mutchler et al. 2008). The concentration of hydroxyl species in the fluid (C_f, f = H_3BO_3, Al, and W) is found using the proportion

$$C_f = \frac{C_{NaCl}}{C_{Na}} \times C_i \qquad (1)$$

where C_{Na} and C_i are the elemental concentrations of Na and species *i* (= B, Al, and W) determined using the elemental method and C_{NaCl} is the concentration of NaCl using the microthermometry method.

FLUID INCLUSIONS

Fluid inclusion types

All samples studied were hosted in quartz and contained abundant inclusions ranging in size from 2 μm to up to 70 μm. Based on appearance and

microthermometry, fluid inclusions were divided into three compositional types. The types correspond to the classification of Sirbescu and Nabelek (2003a):

1. Type 1 are mixed saline aqueous-carbonic fluid inclusions with ice dissolution temperatures from about -20°C to -6°C (Figure 4a and Table 1);
2. Type 2 are saline aqueous inclusions with final dissolution temperatures from about -35°C to 0°C for ice, -20°C to -9°C for hydrohalite, and 9°C to 180°C for halite (Figure 4b);
3. Type 3 fluid inclusions are carbonic, dominated by CO_2 (Figure 4c).

Type 1 fluid inclusions were found in samples from both the Calamity Peak pluton (sample nos. CP-MG8-1, and CP-MG10-1) and from another tourmaline-bearing granite (sample nos. HP-MG5-1) (Figure 2). They are a mixture of H_2O, carbonic fluid, and dissolved salts. The carbonic fluid is dominated by CO_2 with minor CH_4 (Sirbescu and Nabelek 2003a). They are liquid-rich, with two or three phases present at room temperature. The phases include a vapor bubble within a carbonic fluid that is enclosed by an aqueous fluid (Figure 4a). The vapor bubble usually occupies less than 5% of the inclusion volume while the carbonic fluid can occupy up to 70%. They were interpreted as primary from their shape, position, and association with nearby inclusions in the samples: they range in size from 2 to 30 μm, and are usually equant to oblong, sometimes having a negative crystal shape (Figure 4a), and they occur as isolated single inclusions (Figure 4b) or in three-dimensional groups of inclusions (Figure 4c). Type 1 inclusions were interpreted by Sirbescu and Nabelek (2003a) to be representative of the putative magmatic fluid,

trapped when it separated from the HPG magma, because of their association melt inclusion assemblages.

Type 2 inclusions occur in all samples studied (Figure 2). They are saline aqueous inclusions, and are secondary (Sirbescu and Nabelek 2003a). Sirbescu and Nabelek (2003a) divided type 2 inclusions into subtype 2a and 2b. Type 2a have either ice melting temperatures ($T_m$ice) ≥ -21.2°C or $T_m$ice < -21.2°C and halite dissolution temperatures (T_d) ≥ final homogenization temperature (T_h). Type 2b inclusions have a $T_m$ice < -21.2°C and T_d < T_h. Sirbescu and Nabelek (2003a) interpreted type 2 inclusions to be the aqueous phase of the separated type 1 magmatic fluid. Type 2 inclusions are between 2 - 70 μm in diameter and lenticular or irregular in shape (Figure 4d). All type 2 inclusions occur along healed fractures (Figure 4f). They contain two or three phases at room temperature with two-phase inclusions the most common, and consist of a vapor bubble surrounded by an aqueous fluid. Three-phase inclusions also have a solid phase, usually halite at room temperature (Figure 4d).

Type 3 inclusions also occur in most samples (Figure 2). Sirbescu and Nabelek (2003a), described type 3 inclusions as a mixture of CO_2 with a minor amount of CH_4. Type 3 inclusions are secondary, and are interpreted to be the separated carbonic phase of type 1 fluid (Sirbescu and Nabelek 2003a). They are usually irregularly shaped ranging in size from 2 μm up to 15 μm, and occur along healed fractures, sometimes cross-cutting type 2 inclusions. Type 3 fluid inclusions are liquid-rich, with one or two phases present at room temperature. Phases include a carbonic liquid with or without a carbonic vapor phase (Figure 4e). Type

3 inclusions were not analyzed by microthermometry or LA ICP-MS in this study because they contain little aqueous fluid.

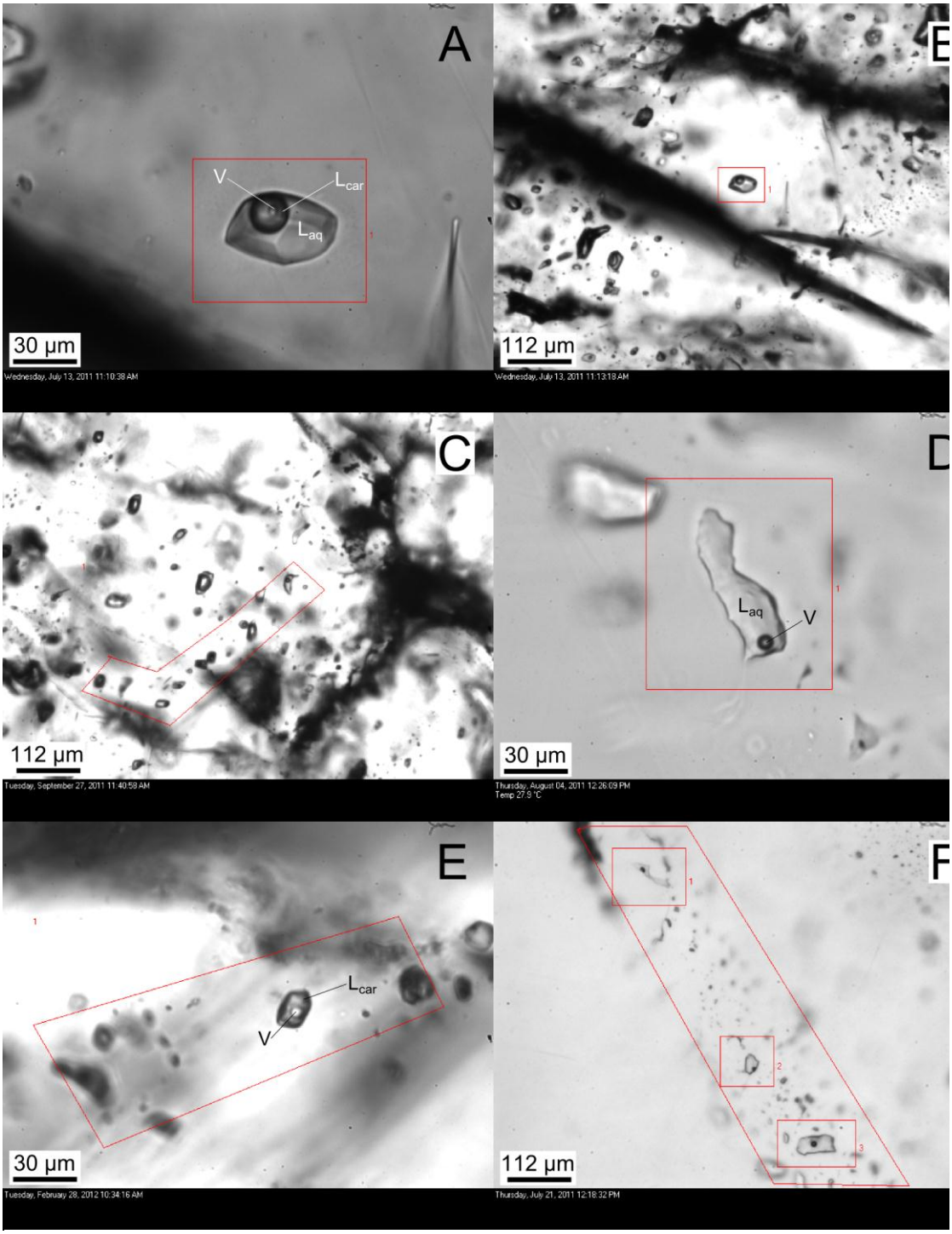

Figure 4. Photomicrographs of quartz-hosted fluid inclusions in the HPG showing the phases present at room temperature: (A) Type 1 (H_2O-CO_2+salt), (B) insolated type 1, (C) three-dimensional array of type 1, (D) type 2 (H_2O+salt), (E) type 3 (CO_2-rich), and (F) type 2 secondary fracture-filling texture.
V--vapor; L_{car}--carbonic liquid; L_{aq}--aqueous liquid.

Microthermometry

Microthermometric data for the two types of fluid inclusions analyzed are summarized in Table 1 and Figure 5a, b, and c. All analyzed type 1 fluid inclusions were hosted in quartz within tourmaline-bearing granites from the Calamity Peak pluton. They have similar thermometric properties: CO_2 melting temperatures vary between -58.4°C and -56.4°C, supporting Sirbescu and Nabelek (2003a) conclusion that CO_2 is the dominant carbonic phase. The dilutant component is thought to be CH_4 because of the low CO_2 melting temperatures and because Sirbescu and Nabelek (2003a) detected methane in type 1 inclusions by raman spectroscopy. Partial homogenization (T_{ph}) to carbonic liquid (L_{car}) plus aqueous liquid (L_{aq}) occurs between 2°C and 32°C, with a majority between 28°C and 30°C. T_h occurs between 200°C and 228°C, with homogenization to liquid. Except for T_h of type 1 inclusions, type 1 and type 2 fluid inclusions encompass a broadly similar microthermometry range to that reported by Nabelek and Ternes (1997) and Sirbescu and Nabelek (2003a). Table 1 also compares the microthermometry data for type 1 and 2 inclusions in this study with those of the above mentioned studies, and shows that our data is in agreement with that of previous studies for type 2 inclusion. T_h for type 1 inclusions analyzed in this study is about 60 to 20°C less than in previous studies.

Type 2 fluid inclusions have greater variation in microthermometric properties, indicating a more complex process involved in their formation. Type 2 inclusions from the "New" pegmatite have high apparent eutectic temperatures between -12.6°C and -11.6°C, which is near the H_2O-KCl eutectic (-10.7°C). Note that

the apparent eutectic temperatures are interpreted to be binary eutectics (T_{be}), since no melting was observed between these temperatures and the final melting temperature. The phase that was melting at the T_{be} could not be identified in these inclusions. Ice was the final phase melting in all inclusions from the tourmaline-absent pegmatite; they are clustered at or near the melting temperature of pure water between -3.4°C and 0.0°C. In contrast, type 2 inclusions from biotite-bearing granites and tourmaline-bearing granites have much lower apparent eutectic temperatures, some as low as -58.4°C. In biotite-bearing granites, T_{be} were between -24.0°C and -21.8°C, with one as low as -36.5°C. In all inclusions from the biotite-bearing granites, hydrohalite was the phase melting at T_{be}, indicating NaCl as the dominate solute, and ice was the final phase melting. For most of the inclusions final ice melting temperatures were between -18.0°C and -9.8°C, but the inclusion with the low T_{be} (-36.5°C) had an ice melting temperature of -27.5°C.

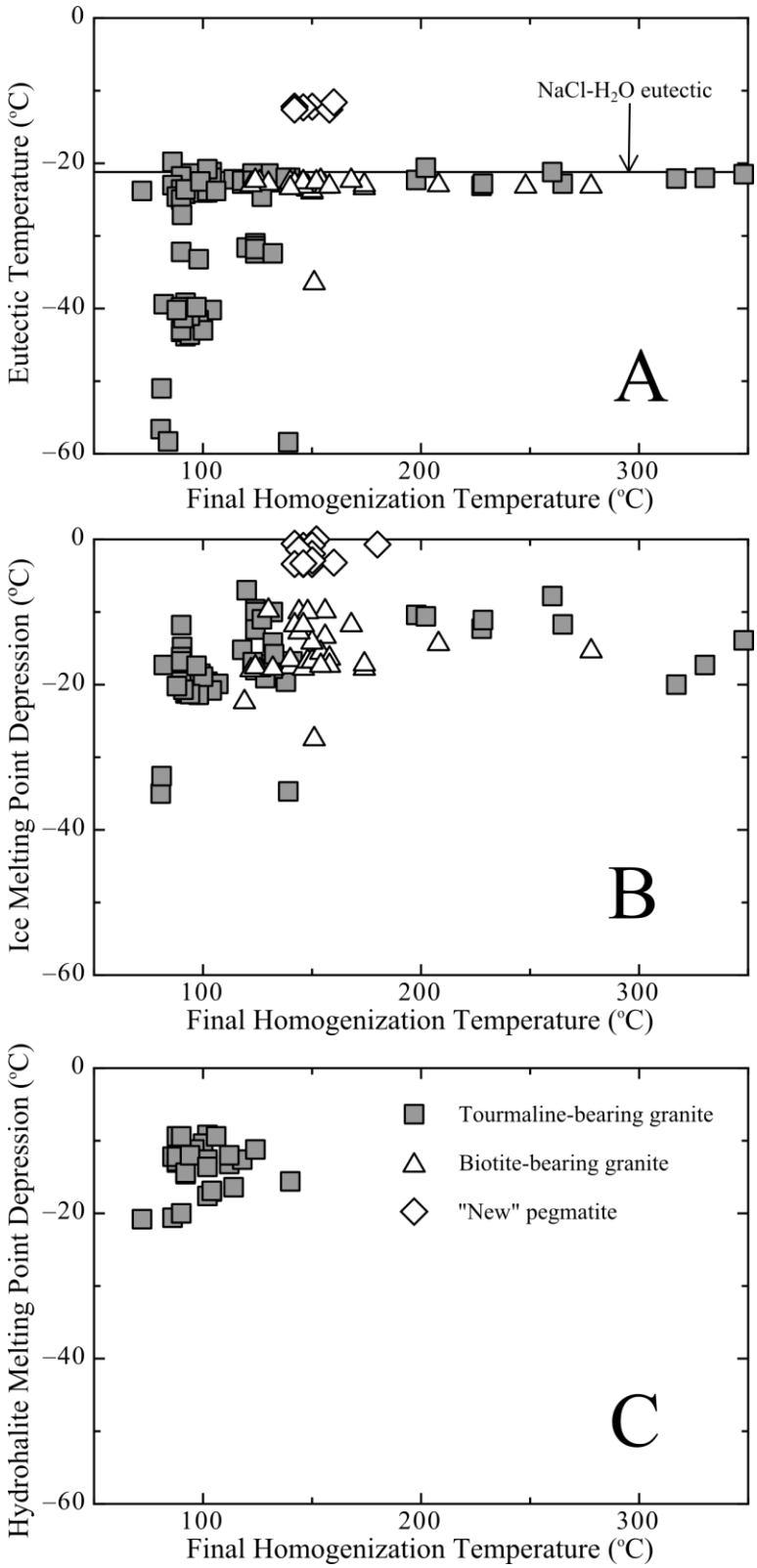

Figure 5. Microthemometric data plotted for type 2 fluid inclusions: (A) apparent eutectic temperature versus final homogenization temperature, (B) ice freezing point depression versus final homogenization temperature, and (C) hydrohalite freezing point depression versus final homogenization temperature.

In tourmaline-bearing granites, six melting relationships were identified based on grouping fluid inclusion assemblages (Figure 6 and Table 1). The general trends include: is a decrease in the final ice melting temperature for relationships A through D, and a decrease in the final hydrohalite temperature for E and F. The first relationship (A) had an unknown phase melting at an apparent ternary eutectic (T_{te}) at -32.5°C. The next phase to melt was hydrohalite, between -32.4°C and -31.0°C, at the apparent T_{be}. The final melting temperature (T_m) was between -12.4°C and -4.2°C, the phase melting was ice. The next relationship (B) had no T_{te} and a higher T_{be} between -27.1°C and -20.6°C with hydrohalite melting. Relationship B had a similar range in T_m as A, with ice melting between -19.6°C and -7.8°C. The next two relationships had very low T_{be}, relationship C between -43.8°C and -33.2°C and relationship D between -58.4°C and -50.2°C. Relationship C had a similar T_m of ice, between -21.4°C and -16.2°C, but relationship D had lower temperatures between -35.0°C and -32.0°C. In the last two melting relationships (E and F; Figure 6), hydrohalite was the final phase melting with T_m between -20.8°C and -9.2°C. Both relationships also had similar T_{be} of ice, between -25.0°C and -19.8°C. Relationship E had T_{te} between -33.6°C and -32.2°C, but relationship F had lower temperatures between -54.2°C and -48.8°C. In only two inclusions from the tourmaline-bearing granites halite was the last phase to melt, with dissolution temperatures of 97.0°C and 148.1°C. Total homogenization to liquid occurs between 80°C and 428°C. The microthermometry data, specifically the low eutectic and melting temperatures, shows that aqueous inclusions are not simple H_2O-NaCl mixtures, but have a more complex solute composition.

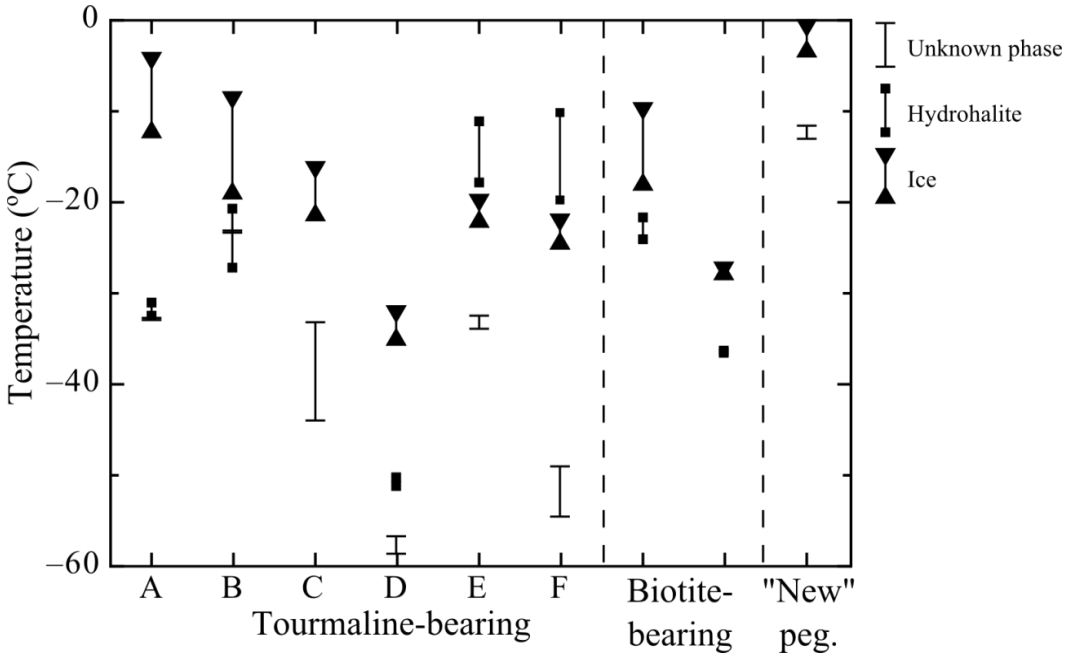

Figure 6. Schematic diagram showing phase transitions observed in Type 2 fluid inclusions in tourmaline- and biotite-bearing granites and the “New” pegmatite. A – F are the six melting relationships found in the tourmaline-bearing granites.

LA ICP-MS results

LA ICP-MS data for Type 1 and Type 2 fluid inclusions from tourmaline-bearing granites and for Type 2 inclusions from biotite-bearing granites and the "New" pegmatite are summarized in Table 2 and Figures 7a and 7b (mean values). The fluid inclusions in each rock type show a pronounced variation in detected elements across the HPG.

1. Tourmaline-bearing granite have NaCl, LiCl, and CsCl detected in type 1, and NaCl, KCl, LiCl, ±Al, ±H_3BO_3, and ±CsCl in type 2 (Figure 7a and 7b) inclusions.
2. Biotite-bearing granite have NaCl, $SrCl_2$, LiCl, ±KCl, and ±$MgCl_2$ detected in their inclusions (Figure 7b).
3. Fluid inclusions in samples from the "New" pegmatite have H_3BO_3, NaCl, Al, LiCl, W, ±KCl, ±RbCl, and ±CsCl detected (Figure 7b).

In tourmaline-bearing granites, the aqueous fluids in the inclusions are dominated by NaCl, KCl, and LiCl. Both type 1 inclusions measured have elevated concentrations of LiCl compared to type 2 inclusions, with the mean about six times higher (0.97 vs. 0.15 wt. %) than the mean concentration in type 2 inclusions. The mean concentration of NaCl in type 1 and type 2 inclusions are nearly the same (20.84 vs. 22.53 wt. %) with type 2 having slightly higher concentrations. KCl was not detected in Type 1 inclusions but it was the second most dominant solute in type 2 inclusions (mean 0.41 wt.%). Also, both type 1 and 2 inclusions contained minor concentrations of CsCl with higher concentrations in type 1 (mean 0.05 wt.

TABLE 2. Summary of LA ICP-MS data for tourmaline-bearing granite, biotite-bearing granite, and the "New" pegmatite. All analysis in wt. % unless otherwise noted.

Sample ID	Chip	Inclusion & Rock* Type		LiCl	H_3BO_3	NaCl	$MgCl_2$	Al	KCl	RbCl	$SrCl_2$	CsCl	$BaCl_2$	W	Total Salinity ($NaCl_{eq}$)
CP9-3B FI2	2a	2	Tur	0.14		23.33			0.22	<DL†		<DL†			23.7
CP9-3B FI3	2a	2	Tur	0.17		23.32			0.20	<DL†		<DL†			23.7
CP9-3B FI4	2a	2	Tur	0.14		23.36			0.25	<DL†		<DL†			23.8
CP9-3B FI7	2a	2	Tur	0.14		23.23		0.02	0.13	<DL†		<DL†			23.6
CP9-3B FI8	2a	2	Tur	0.21		22.83			0.65	<DL†		0.01			23.7
CP9-3B FI10	2a	2	Tur	0.16		22.67			0.27	<DL†		0.01			23.1
CP9-3B FI11	2a	2	Tur	0.20		22.68			0.48	<DL†		<DL†			23.4
CP9-3B FI15a	2a	2	Tur	0.13		22.51			0.32	<DL†		<DL†			23.0
CP9-3B FI15b	2a	2	Tur	0.14		22.35			0.47	<DL†		<DL†			23.0
CP9-3B FI17	3	2	Tur	0.14	0.02	20.99	<DL†		0.33	<DL†	<DL†				21.5
CP9-3B FI19	3	2	Tur	0.15		21.39			0.55	<DL†	<DL†				22.1
CP9-3B FI21	3	2	Tur	0.09		22.24			0.83	<DL†	<DL†				23.2
CP9-3B FI22	3	2	Tur	0.14		21.94			0.69	<DL†	<DL†				22.8
CP-MG8-1 FI11	1	1	Tur	1.65		19.99						0.03			21.7
CP-MG8-1 FI16	1	1	Tur	0.28		21.69						0.06			22.0
HP-MG4-1 FI21	1	2	Bt	0.33		24.62			1.08	<DL†	0.26	<DL†	<DL†		26.3
HP-MG4-1 FI23	1	2	Bt	0.17		24.88	0.86				0.35	<DL†			26.3
HP-MG1-1 FI1	1	2	"New"	0.25	4.71	3.00		0.37	1.38	0.01		0.01		0.02	4.7
HP-MG1-1 FI13	1	2	"New"	0.73	2.91	2.66		0.11				<DL†		0.01	3.4

* Tur—tourmaline-bearing granite, Bt—biotite-bearing granite, "New"—"New" pegmatite.

† <DL—less than detection limit.

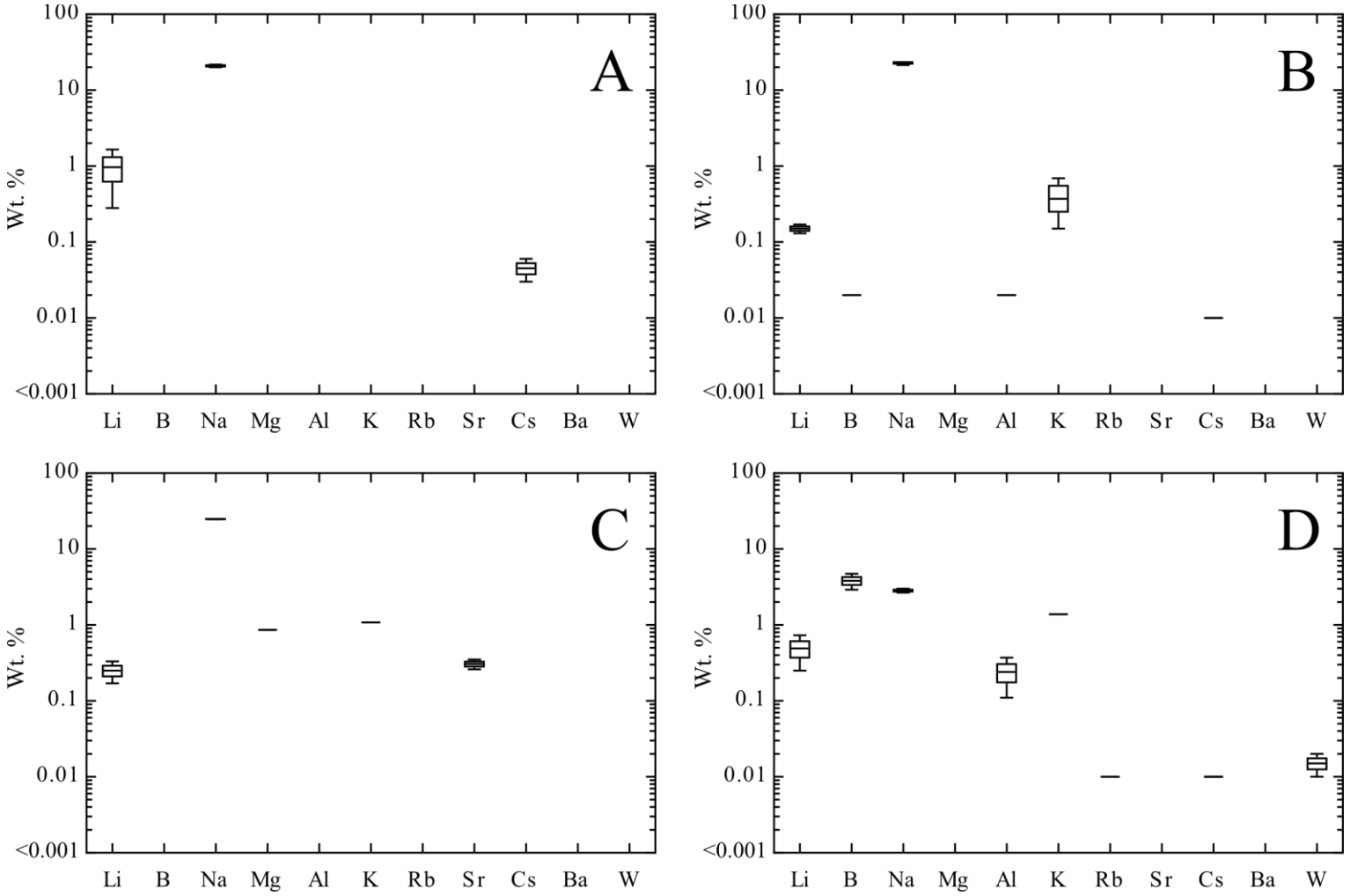

Figure 7. Fluid inclusion LA ICP-MS data showing detected elements: (A) type 1 and (B) type 2 inclusions in tourmaline-bearing granites, (C) type 2 inclusions in biotite-bearing granites, and (D) type 2 inclusions in the "New" pegmatite.

%) than in type 2 inclusions (≤0.01 wt. %). In addition, type 2 inclusions had one inclusion with Al (~0.02 wt. %) and another inclusion with H_3BO_3 (~0.02 wt. %), but from the LA ICP-MS spectral signal none of the other inclusions appeared to contain either of these solutes. Some type 2 inclusions contained Rb and Sr based on their ICP-MS signal being above the background, but the concentrations were below the 3-sigma (3σ) detection limits.

Both fluid inclusions in biotite-bearing granites were dominated by NaCl (mean 24.75 wt. %), $SrCl_2$ (mean 0.31 wt. %), and LiCl (mean 0.25 wt. %), but one contained major concentrations of KCl (1.08 wt. %) and the other contained high concentrations of $MgCl_2$ (0.86 wt. %). The inclusion containing KCl also produced Rb, Cs, and Ba signals, but the concentrations were below 3σ detection limits. KCl may not have been detected in the other inclusion because of a high background signal during the analysis (Figure 3).

Fluid inclusions in the "New" pegmatite are dominated by H_3BO_3, NaCl, Al, and LiCl. NaCl concentrations are low (mean 2.83 wt. %), especially in comparison with inclusions in the granites, but H_3BO_3 concentrations are much higher (mean 3.81 wt. %). LiCl concentrations however are the same or only slightly elevated in the "New" pegmatite compared to the granites. Both fluid inclusions in the "New" pegmatite also contained significant concentrations of Al (mean 0.93 wt. %). One of the inclusions contained major concentrations of KCl (1.38 wt. %), but in the other inclusion KCl was not detected. Both inclusions contained minor concentrations of CsCl (≤0.01 wt. %) and W (≤0.02 wt. %).

There are systematic differences between fluid inclusions in the three sets of rocks analyzed. The most apparent differences are in salinity. The tourmaline-bearing granites have salinities that range from 23.8 to 21.5 wt. % $NaCl_{eq}$, and the biotite-bearing granite have salinities that are slightly higher both inclusions at 26.3 wt. % $NaCl_{eq}$. In contrast, "New" pegmatite salinities are only 4.6 and 3.4 wt. % $NaCl_{eq}$. The range in salinities of type 2 inclusions could be attributed to trapping of the fluid in the immiscibility field in the H_2O-$NaCl_{eq}$ system.

DISCUSSION

One of the main goals of this study was to determine the role that the magmatic fluids played in the differentiation of the HPG and in metasomatism of its aureole. The data from microthermometry and LA ICP-MS analysis of fluid inclusions provides evidence for the complex melt and fluid evolution of the HPG system. Previous studies have interpreted type 1 (H_2O-CO_2+salts) inclusions as representing the original magmatic fluid exsolved from the HPG magma, and type 2 (H_2O+salts) and that type 3 (CO_2-rich) fluid inclusions were trapped after the original magmatic fluid unmixed (Nabelek and Ternes 1997; Sirbescu and Nabelek 2003a). In the present study, the data shows the preference of B and other elements carried as hydroxyls for the low salinity vapor over a higher salinity fluid. First, using microthermometry and LA ICP-MS data, the composition of the fluid inclusions in the context of their variation across the HPG pluton will be discussed, in comparison with previously published fluid inclusion work in the study area. Second, the inclusion data will be used to estimate concentration of Li in the HPG magma, and what are the implications for the evolution of the HPG. The inclusion

data will be discussed in the context of the enrichment of certain elements in the contact aureole.

Variations of composition in the fluid

Fluid inclusions in the tourmaline- and biotite-bearing granites have similar compositions for NaCl, but there are some very important differences (Figure 7 and 8). Figure 7a, b, and c shows that the mean concentrations of NaCl for all types of inclusions in both granites are remarkably similar. In the tourmaline-bearing granites, type 2 inclusions have similar concentrations of KCl to those of biotite-bearing granites and in the "New" pegmatite, but type 1 inclusions lack KCl (Figure 7 and 9). This is probably because either type 2 inclusions equilibrated with potassium feldspar or K was not detected in type 1 inclusions because of a high background signal (see Figure 3). KCl concentrations in the fluid in the biotite-bearing granite are higher than in the tourmaline-bearing granite probably because of a higher chloride content. LiCl (Figure 7a and b) concentrations, however, have similar ranges between the type 1 and type 2 fluid inclusions in the granites. Only one type 1 inclusion contained a higher amount of LiCl than any of the type 2 inclusions in tourmaline-bearing granites. In addition, type 1 inclusions contain a higher amount of CsCl than any of the type 2 inclusions in tourmaline-bearing granites (Table 2 and Figure 7). This is surprising since Webster et al. (1989) showed that in mixed H_2O-CO_2 fluids Li and Cs partition into the melt. Type 2 fluid inclusions in the biotite-bearing granite have a similar LiCl concentration to the tourmaline-bearing granites suggesting that the magmas had similar Li concentrations or the inclusions represent subsolidus equilibration with the granites. Fluid inclusions in the

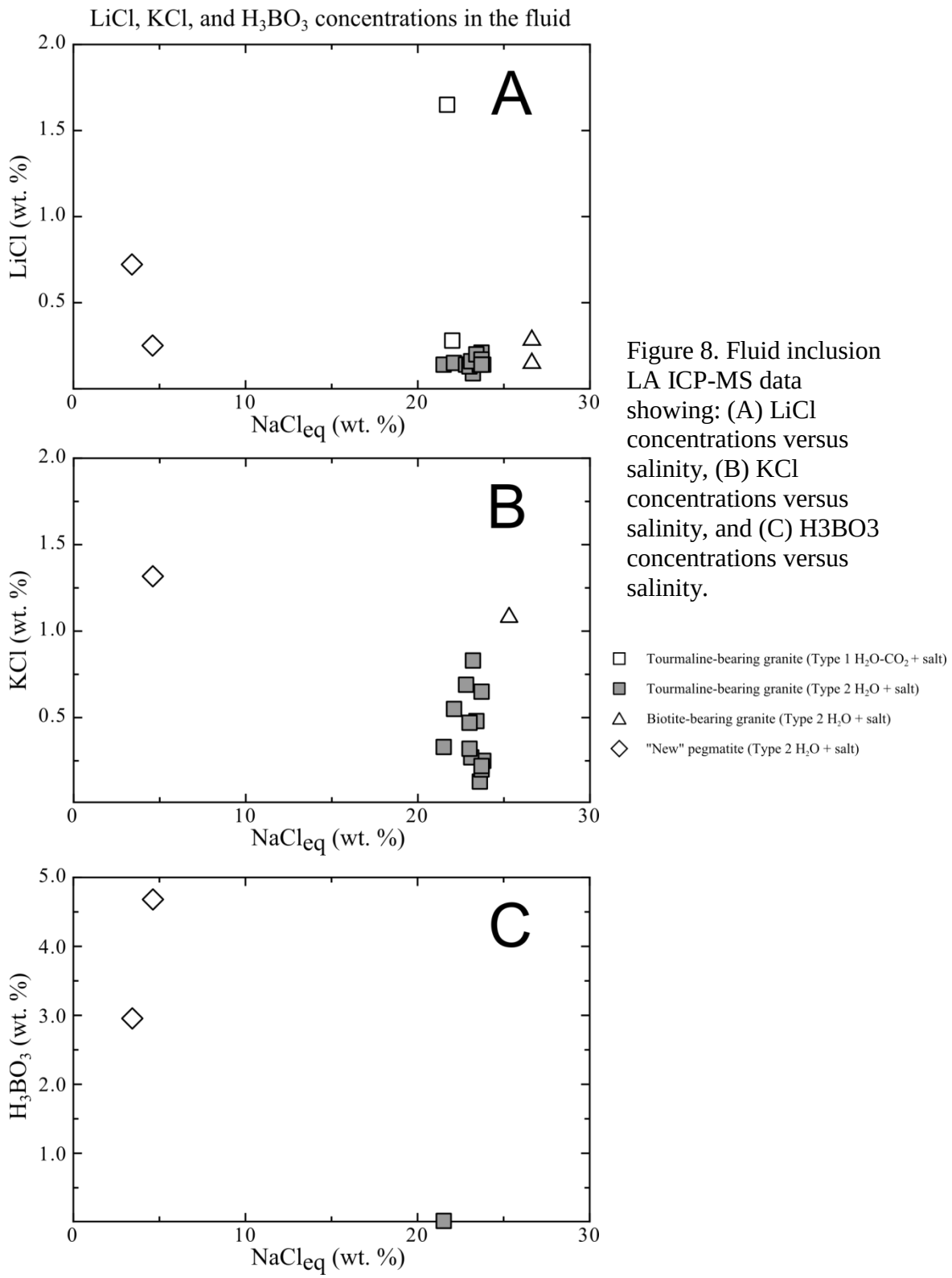

Figure 8. Fluid inclusion LA ICP-MS data showing: (A) LiCl concentrations versus salinity, (B) KCl concentrations versus salinity, and (C) H3BO3 concentrations versus salinity.

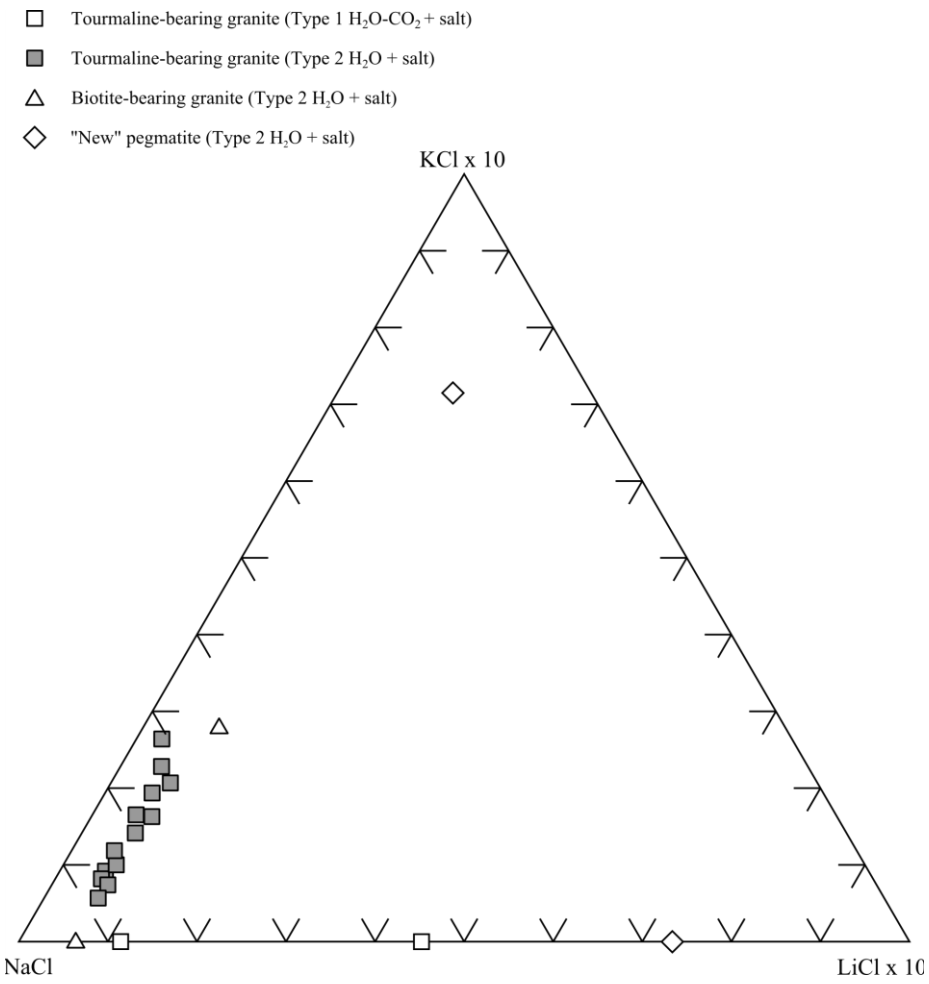

Figure 9. NaCl-LiClx10-KClx10 ternary diagram (wt. %) showing type 2 fluid inclusions from biotite-bearing granite, "New" pegmatite, and types 1 and 2 from tourmaline-bearing granite.

biotite-bearing granite also have some $SrCl_2$; this makes sense because the data from Nabelek et al. (1992a) for biotite-bearing granites have higher Sr content. What is unusual, however, is that Sr was not detected in any of the fluid inclusions in the tourmaline-bearing granite. Webster et al. (1989) showed that Sr partitioning depends strongly on the Cl concentration. Since the difference in the salinity in the fluid inclusions and the Sr concentrations in the granites (biotite-bearing: up to 88 ppm Sr;

tourmaline-bearing: up to 72 ppm Sr; Nabelek et al. 1992a) are not great the reason for Sr to be in the biotite-bearing and not the tourmaline-bearing granite is unknown.

Compared to the tourmaline- and biotite-bearing granites, fluid inclusions in the "New" pegmatite have very different compositions. The concentration of NaCl is ~10 times lower in the "New" pegmatite inclusions than in either the tourmaline- or biotite-bearing granites (Figure 7d). In both inclusions, LiCl is slightly elevated when compared with fluids in both granites (Figure 8a), and KCl concentrations are higher than in the tourmaline- or biotite-bearing granite (Figure 8b and 9). Figure 8c shows that fluid inclusions in the "New" pegmatite have H_3BO_3 concentrations that are about 100 times the content from one inclusion in the tourmaline-bearing granite in which B was detected. This data supports Schatz et al. (2004) study indicating that B prefers the low salinity fluid. It also explains metasomatic tourmaline found in the contact aureole of the "New" pegmatite. Also, fluid inclusions in the "New" pegmatite contain W and higher concentrations of Al. This may suggest that low salinity B-rich fluids can mobilize W and possibly Al.

Li concentration in the Harney Peak Granite

Using the composition of LiCl and in the fluid, one can estimate the concentration of Li in the HPG melt when the fluid was trapped. When considering Li and other chloride complexes, the partitioning behavior of Cl must be considered. The partitioning of LiCl was estimated using the results of Webster et al. (1989). Webster et al. (1989) determined the partition coefficient of Li ($D_{Li}^{f/m}$) in topaz rhyolite melt at variable Cl concentrations. The appropriate $D_{Li}^{f/m}$ for the HPG was estimated from the measured

concentration of Cl in the fluid inclusions. The concentration of Cl in the fluid (C_{Cl}^{f}) can be estimated by

$$C_{Cl}^{f} = \sum C_{MCl}^{f} \times X_{Cl}^{MCl} \qquad (4)$$

where C_{MCl}^{f} is the concentration of MCl (M = Li, Na, K, Rb, Cs, etc.) detected in the fluid, and X_{Cl}^{MCl} is the mass fraction of M in MCl. The concentration of Li (C_{Li}^{f}) in the fluid is calculated in the same way

$$C_{Li}^{f} = C_{LiCl}^{f} \times X_{Li}^{LiCl} \qquad (5)$$

where C_{LiCl}^{f} is the concentration of LiCl in the fluid, and X_{Li}^{LiCl} is the mass fraction of Li in LiCl. Thus, the estimated concentration of Li in the fluid is 3000 to 500 (type 1) for tourmaline-bearing granite. The concentration of Li in the coexisting melts (C_{Li}^{m}) were calculated using

$$D_{Li}^{f/m} = \frac{C_{Li}^{f}}{C_{Li}^{m}} \qquad (6)$$

where $D_{Li}^{f/m}$ is the equilibrium partition coefficient of Li between fluid and the granitic melt. Using type 1 inclusions in the tourmaline-bearing granite, the concentration in the melt is 2000 and 300 ppm Li. The values are much higher than the concentrations estimated by Wilke et al. (2002) (~12 to 18 ppm Li), which suggests origin of Li is more complex than simple partial melting of the metasediments in the Black Hills.

Li and B concentrations in the contact aureole

LA ICP-MS data collected for this study support the hypothesis that the enrichment of Li in the HPG contact aureole is due to interaction with fluids emanating from the HPG and associated pegmatites (Wilke et al. 2002). Wilke et al. (2002) found the spatial distribution of B in the contact aureole followed no apparent pattern, and the concentration of B and Li appeared independent of metamorphic grade. In contrast, Li concentrations did have a spatial pattern consistent with the concentration of Li decreasing with distance from the center of the pluton. Wilke et al. (2002) hypothesized that the enrichment was caused by fluids emanating from the HPG. They determined the concentration of Li in the contact aureole is up to ~250 ppm (Wilke et al. 2002), data from this study shows that all fluid inclusions sampled contained Li in high enough concentrations (~150 to 3000 ppm Li) to account for the Li in the contact aureole.

CONCLUSIONS

1) The results show all fluid inclusions measured by LA ICP-MS have elevated concentrations of LiCl, indicating that the magmatic fluid from the HPG magma contained significant amounts of Li. The data supports the hypothesis of Sirbescu and Nabelek (2003a) and Wilke et al. (2002) that magmatic fluids emanating from the HPG caused enrichment of Li in the contact aureole.
2) Elevated concentrations of B are only found in fluid inclusions from the "New" pegmatite. This supports experimental work that suggests that fluids need to have low salinity to be able to mobilize B (Schatz et al. 2004).

3) Type 1 and type 2 fluid inclusions have different aqueous fluid compositions. Higher concentrations of LiCl and CsCl are in type 1 fluids than in type 2, but both have nearly the same concentration of NaCl. Type 2 fluids have elevated KCl, which could be explained by the exchange of K with potassium feldspar at subsolidus conditions.
4) Fluid inclusions in the "New" pegmatite provide evidence that W partitions into B-rich fluids, which correlates with the frequent association of tourmaline and W deposits (Schatz et al. 2004).

REFERENCES CITED

Bartels, Alexander, Francesco Vetere, Francois Holtz, Harald Behrens, and Robert L. Linnen. 2010. Viscosity of flux-rich pegmatitic melts. *Contributions to Mineralogy and Petrology* 162 (1):51-60.

Bodnar, R. J. 2003. Reequilibration of fluid inclusions. In *Fluid Inclusions: Analysis and Interpretation*, edited by I. Samson, A. Anderson and D. Marshall: Mineralogical Association of Canada.

Dahl, Peter S., and Robert Frei. 1998. Step-leach Pb-Pb dating of inclusion-bearing garnet and staurolite, with implications for Early Proterozoic tectonism in the Black Hills collisional orogen, South Dakota, United States. *Geology* 26 (2):111-114.

Dahl, Peter S., Michael A. Hamilton, Michael J. Jercinovic, Michael P. Terry, Michael L. Williams, and Robert Frei. 2005a. Comparative isotopic and chemical geochronometry of monazite, with implications for U-Th-Pb dating by electron microprobe: An example from metamorphic rocks of the eastern Wyoming Craton (U.S.A.). *American Mineralogist* 90 (4):619-638.

Dahl, Peter S., Michael P. Terry, Michael J. Jercinovic, Michael L. Williams, Michael A. Hamilton, Kenneth A. Foland, Susanne M. Clement, and LaVerne M. Friberg. 2005b. Electron probe (Ultrachron) microchronometry of metamorphic monazite: Unraveling the timing of polyphase thermotectonism in the easternmost Wyoming Craton (Black Hills, South Dakota). *American Mineralogist* 90 (11-12):1712-1728.

Duke, Edward F. 1995. Contrasting scales of element mobility in metamorphic rocks near Harney Peak Granite, Black Hills, South Dakota. *Geological Society of America Bulletin* 107 (3):274-285.

Duke, Edward F., Jack A. Redden, and James J. Papike. 1988. Calamity Peak layered granite-pegmatite complex, Black Hills, South Dakota: Part I. Structure and emplacement. *Geological Society of America Bulletin* 100 (6):825-840.

Duke, Edward F., C. K. Shearer, Jack A. Redden, and James J. Papike. 1990. Proterozoic Granite-Pegmatite Magmatism, Black Hills, South Dakota: Structure and Geochemical Zonation. In *The Early Proterozoic Trans-Hudson Orogen of North America*, edited by J. F. Lewry and M. R. Stauffer: Geological Association of Canada.

Gleeson, Sarah A. 2003. Bulk analysis of electrolytes in fluid inclusions. In *Fluid Inclusions: Analysis and Interpretation*, edited by I. Samson, A. Anderson and D. Marshall: Mineralogical Association of Canada.

Heinrich, C. A., T. Pettke, W. E. Halter, M. Aigner-Torres, A. Audétat, D. Günther, B. Hattendorf, D. Bleiner, M. Guillong, and I. Horn. 2003. Quantitative multi-element analysis of minerals, fluid and melt inclusions by laser-ablation inductively-coupled-plasma mass-spectrometry. *Geochimica et Cosmochimica Acta* 67 (18):3473-3497.

Helms, Thomas S., and Theodore C. Labotka. 1991. Petrogenesis of Early Proterozoic pelitic schists of the southern Black Hills, South Dakota: Constraints on regional low-pressure metamorphism. *Geological Society of America Bulletin* 103:1324-1334.

Lange, Rebecca A. 1994. The effect of H_2O, CO_2 and F on the density and viscosity of silicate melts. *Reviews in Mineralogy and Geochemistry* 30:331-370.

Maloney, Jennifer S., Peter I. Nabelek, Mona-Liza C. Sirbescu, and Ralf Halama. 2008. Lithium and its isotopes in tourmaline as indicators of the crystallization process in the San Diego County pegmatites, California, USA. *European Journal of Mineralogy* 20 (5):905-916.

Mutchler, S. R., L. Fedele, and R. J. Bodnar. 2008. Analysis management system (AMS) for reduction of laser ablation ICP-MS data. In *Laser-Ablation-ICPMS in the Earth Sciences: Current Practices and Outstanding Issues*, edited by P. Sylvester: Mineralogical Association of Canada Short Course Series.

Nabelek, Peter I., Theodore C. Labotka, Thomas S. Helms, and Max Wilke. 2006. Fluid-mediated polymetamorphism related to Proterozoic collision of Archean Wyoming and Superior provinces in the Black Hills, South Dakota. *American Mineralogist* 91 (10):1473-1487.

Nabelek, Peter I., and Mian Liu. 2004. Petrologic and thermal constraints on the origin of leucogranites in collisional orogens. *Transactions of the Royal Society of Edinburgh: Earth Sciences* 95 (1-2):73-85.

Nabelek, Peter I., Carol Russ-Nabelek, and J. R. Denison. 1992a. The generation and crystallization conditions of the Proterozoic Harney Peak Leucogranite, Black Hills, South Dakota, USA: Petrologic and geochemical constraints. *Contributions to Mineralogy and Petrology* 110 (2-3):173-191.

Nabelek, Peter I., Carol Russ-Nabelek, and G. T. Haeussler. 1992b. Stable isotope evidence for the petrogenesis and fluid evolution in the Proterozoic Harney Peak leucogranite, Black Hills, South Dakota. *Geochimica et Cosmochimica Acta* 56 (1):403-417.

Nabelek, Peter I., and Kim Ternes. 1997. Fluid inclusions in the Harney Peak Granite, Black Hills, South Dakota, USA: Implications for solubility and evolution of magmatic volatiles and crystallization of leucogranite magmas. *Geochimica et Cosmochimica Acta* 61 (7):1447-1465.

Nabelek, Peter I., Alan G. Whittington, and Mona-Liza C. Sirbescu. 2010. The role of H_2O in rapid emplacement and crystallization of granite pegmatites: resolving the paradox of large crystals in highly undercooled melts. *Contributions to Mineralogy and Petrology* 160 (3):313-325.

Norton, James J., and Jack A. Redden. 1990. Relations of zoned pegmatites to other pegmatites, granite, and metamorphic rocks in the southern Black Hills, South Dakota. *American Mineralogist* 75 (5-6):631-655.

Redden, Jack A., Z. E. Peterman, R. E. Zartman, and E. DeWitt. 1990. U-Th-Pb Geochronology and Preliminary Interpretation of Precambrian Tectonic Events in the Black Hills, South Dakota. In *The Early Proterozoic Trans-Hudson Orogen of North America*, edited by J. F. Lewry and M. R. Stauffer: Geological Association of Canada.

Rockhold, J. R., Peter I. Nabelek, and Michael D. Glascock. 1987. Origin of rhythmic layering in the Calamity Peak satellite pluton of the Harney Peak Granite, South Dakota: The role of boron. *Geochimica et Cosmochimica Acta* 51 (3):487-496.

Schatz, Oliver J, David Dolejš, John Stix, Anthony E William-Jones, and Graham D Layne. 2004. Partitioning of boron among melt, brine and vapor in the system haplogranite-H_2O-NaCl at 800 °C and 100 MPa. *Chemical Geology* 210 (1-4):135-147.

Sirbescu, Mona-Liza C., and Peter I. Nabelek. 2003a. Crystallization conditions and evolution of magmatic fluids in the Harney Peak Granite and associated pegmatites, Black Hills, South Dakota–Evidence from fluid inclusions. *Geochimica et Cosmochimica Acta* 67 (13):2443-2465.

———. 2003b. Crustal melts below 400°C. *Geology* 31 (8):685-688.

Webster, J. D., J. R. Holloway, and R. L. Hervig. 1989. Partitioning of Lithophile Trace Elements between H2O and H2O + CO2 Fluids and Topaz Rhyolite Melt. *Economic Geology* 84:116-134.

Whittington, Alan G., Bridget M. Hellwig, Harald Behrens, Bastian Joachim, André Stechern, and Francesco Vetere. 2009. The viscosity of hydrous dacitic liquids: implications for the rheology of evolving silicic magmas. *Bulletin of Volcanology* 71 (2):185-199.

Wilke, Max, Peter I. Nabelek, and Michael D. Glascock. 2002. B and Li in Proterozoic metapelites from the Black Hills, U.S.A.: Implications for the origin of leucogranitic magmas. *American Mineralogist* 87 (4):491-500.